SAND2021-0424C

Proceedings of the ASME 2020 Pressure Vessels & Piping Conference
PVP 2020
July 19-24, 2020, Minneapolis, MN, USA

PVP2020-21263

MEASURING FATIGUE CRACK GROWTH BEHAVIOR OF FERRITIC STEELS NEAR THRESHOLD IN HIGH PRESSURE HYDROGEN GAS

Joseph Ronevich[1], Chris San Marchi[1], Kevin A. Nibur[2], Paolo Bortot[3], Gianluca Bassanini[3], Michele Sileo[3]
[1]Sandia National Laboratories, Livermore, CA, USA
[2]Hy-Performance Materials Testing, LLC., Bend, OR, USA
[3]Tenaris-Dalmine, Dalmine, Italy

ABSTRACT

Following the ASME codes, the design of pipelines and pressure vessels for transportation or storage of high-pressure hydrogen gas requires measurements of fatigue crack growth rates at design pressure. However, performing tests in high pressure hydrogen gas can be very costly as only a few laboratories have the unique capabilities. Recently, Code Case 2938 was accepted in ASME Boiler and Pressure Vessel Code (BPVC) VIII-3 allowing for design curves to be used in lieu of performing fatigue crack growth rate (da/dN vs. ΔK) and fracture threshold (K_{IH}) testing in hydrogen gas. The design curves were based on data generated at 100 MPa H_2 on SA-372 and SA-723 grade steels; however, the data used to generate the design curves are limited to measurements of ΔK values greater than 6 MPa $m^{1/2}$. The design curves can be extrapolated to lower ΔK (<6 MPa $m^{1/2}$), but the threshold stress intensity factor (ΔK_{th}) has not been measured in hydrogen gas. In this work, decreasing ΔK tests were performed at select hydrogen pressures to explore threshold (ΔK_{th}) for ferritic-based structural steels (e.g. pipelines and pressure vessels). The results were compared to decreasing ΔK tests in air, showing that the fatigue crack growth rates in hydrogen gas appear to yield similar or even slightly lower da/dN values compared to the curves in air at low ΔK values when tests were performed at stress ratios of 0.5 and 0.7. Correction for crack closure was implemented, which resulted in better agreement with the design curves and provide an upper bound throughout the entire ΔK range, even as the crack growth rates approach ΔK_{th}. This work gives further evidence of the utility of the design curves described in Code Case 2938 of the ASME BPVC VIII-3 for construction of high pressure hydrogen vessels.

NOMENCLATURE

a	=	crack length, precrack length
a/W	=	crack length/width
ACR	=	adjusted compliance ratio
B, B_N	=	specimen thickness: actual, effective
b_o	=	remaining ligament
CT	=	compact tension
FCGR	=	fatigue crack growth rate
K	=	stress intensity factor
K_{IH}	=	fracture threshold in hydrogen
ΔK_{ACR}	=	closure corrected stress intensity factor range
ΔK_{th}	=	threshold stress intensity factor
TL	=	transverse-longitudinal
UTS	=	ultimate tensile strength
W	=	width
YS	=	yield strength

Sandia National Laboratories is a multimission laboratory managed and operated by National Technology & Engineering Solutions of Sandia, LLC, a wholly owned subsidiary of Honeywell International Inc., for the U.S. Department of Energy's National Nuclear Security Administration under contract DE-NA0003525.

INTRODUCTION

Hydrogen is transported and stored in ferritic steel infrastructure safely. These technologies have been in place for many decades even though ferritic steels can be severely embrittled by hydrogen. However, broad distribution of hydrogen for the transportation sector shifts the infrastructure into a different operational state that is much more exposed to pressure fluctuations and brings these technologies closer to the public. For example, a hydrogen pipeline that services a petrochemical refinery can be operated at constant pressures as the demand is constant; however, stationary storage pressure vessels at hydrogen refueling stations on commercial street corners are subjected to fluctuations in pressure that match the demand of the consumers. The local capacity at a refueling station is not sufficient to maintain constant pressure during vehicle fills and the consequence is fatigue loading of the pressure vessels.

High pressure vessels, such as those used in hydrogen refueling stations, are designed according to the ASME Boiler and Pressure Vessel Code Section VIII Division 3 (BPVC VIII-3), and require both fatigue crack growth rate and fracture toughness (K_{IH}) measurements in the service environment, in this case hydrogen pressure up to 100 MPa. Recently, Code Case 2938 was approved which allows for use of the design curves in lieu of performing fatigue crack growth rate and K_{IH} testing in high pressure hydrogen gas. The development of design curves were based on the best available data generated at > 100 MPa H_2 as described previously [1], which were collected at ΔK of 6 MPa $m^{1/2}$ and higher. Since data were not collected at values below ΔK of 6 MPa $m^{1/2}$, linear extrapolation is needed and therefore an assumption is made that there is no fatigue crack growth threshold, ΔK_{th}. A ΔK_{th} most likely exists, and therefore, the design curves can be overly conservative and limit the design life of the vessel. In addition, often times the high-pressure tanks are operated using a cascade type approach in which the tanks are operated over a narrow pressure range. Often times the tanks are refilled without dropping to their minimum pressure resulting in relatively low ΔK for that given cycle (i.e., ΔK < 6 MPa $m^{1/2}$). Depending on the flaw size, operating pressure, and dimensions of the vessel, early stages of vessel life could exist in this low ΔK regime where no data have been generated to date. Additionally, the majority of the life of a pressure vessel exists at the lower ΔK values, thus overly conservative assumptions in this regime can results in unnecessarily short design life. This current study is motivated by the desire to ensure the best design data are available to optimize design life calculations.

Measuring fatigue crack growth rates in the low ΔK regime is quite challenging in that these tests require arduously long test times if performed at appropriate (low) test frequencies. Even at a relatively high frequency of 10 Hz, tests require multiple weeks to acquire sufficient data to characterize the behavior at the low da/dN range. In this paper, fatigue crack growth rates were measured in high pressure hydrogen gas in the low ΔK range (ΔK < 6 MPa $m^{1/2}$) at a frequency of 10 Hz for ferritic steels. The effects of stress ratio and pressure are examined in comparison to data collected in air.

EXPERIMENTAL PROCEDURES

Materials

An ASME SA372 Grade J material was examined, which is representative of the materials commonly used in high pressure storage tanks for hydrogen refueling stations. The ASME SA372 Gr. J material had a yield strength (YS) of 760 MPa and an ultimate tensile strength (UTS) of 890 MPa. The microstructure of the SA372 Grade J material is shown in Fig. 1a which consists of quenched and tempered martensite with carbides distributed throughout the martensite. Two additional pressure vessel steels were considered in this study for comparison: 4130X (DOT-3AAX) and ASTM A372 Grade N. Class 100 steel. We did not obtain micrographs of their microstructure. However, broadly speaking, the microstructure of both materials is assumed to be quenched and tempered martensite. The 4130X has a yield strength of 641 MPa and UTS of 786 MPa. The minimum requirements for ASTM A372 Grade N Class 100 are YS > 690 MPa and UTS between 795 and 965 MPa.

A high strength pipeline steel grade, API 5L X100, was also examined in this study. This material has a longitudinal YS of 732 MPa and a UTS of 868 MPa. The microstructure of the X100 steel is shown in Fig. 1b consisting of ferrite and bainite. The compositions for X100, SA372 Grade J, and 4130X can be found in Table 1. The composition of the A372 Grade N Class 100 steel was not measured but the ranges are shown in Table 1.

Specimen Preparation

Compact tension (CT) specimens were extracted from the steel vessels and pipes in the CL orientation (commonly described as the TL), such that the load would be applied consistent with the hoop direction (C) and the crack would advance in the axial direction (L). Specimens were machined according to ASTM E647 [2] with a width (W)

of 26.4 mm, thickness (B) of 12.7 mm, a notch length to width ratio of 0.2. Additionally side grooves were machined to a reduced thickness (B_N) of 11.2 mm. Specimens were precracked in air in two stages: compression-compression precracking to initiate a crack followed by tension-tension precracking to advance the crack [3]. The compression-compression precracking was accomplished through rigid test fixtures and pin loading in compression to minimum loads of -13.3 kN (-3,000 lbf) at a stress ratio R=0.05. This procedure typically initiated and advanced the crack approximately 0.2 mm. Subsequent tension-tension precracking was used to extend the crack an additional 3-5 mm at K_{max} values of 11 MPa $m^{1/2}$ at R=0.1 to final crack length to width ratio (a/W) in the range of 0.34 to 0.38.

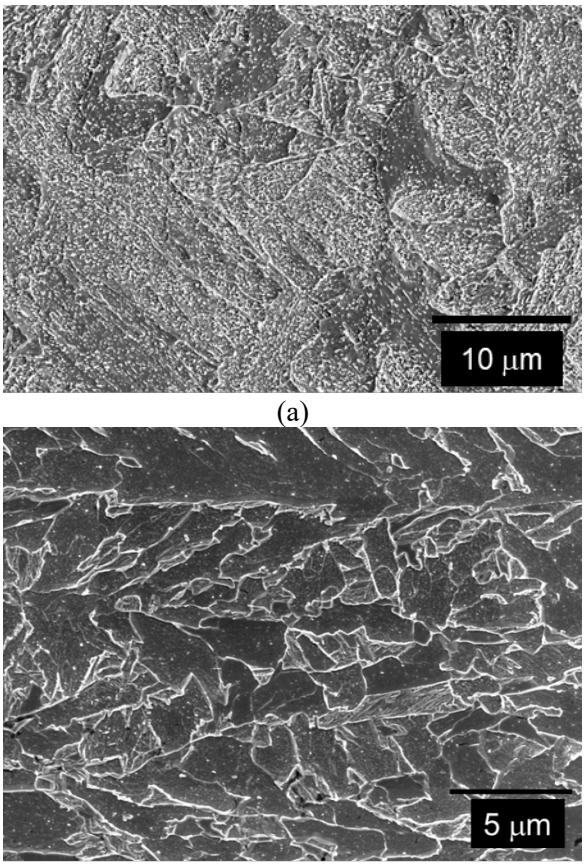

(a)

(b)

Figure 1 – Scanning electron microscope images of (a) SA372 Grade J, (b) X100 pipeline steel. Etched 2% nital.

Fatigue Crack Growth Rate Measurements

Tests were executed in K-control under decreasing K-gradient (e.g. K-shed conditions), where K is the stress intensity factor. As the goal of this work was to measure the low ΔK-regime, a frequency of 10 Hz was used to make test duration manageable. In addition, the K-gradient [2] was controlled at either -0.31 or -0.39 mm^{-1} to help reduce test time. Despite these efforts to reduce test duration, each fatigue crack growth rate (FCGR) curve at each stress ratio required over 1 week to complete. Tests were completed at stress ratios (R) of 0.5 and 0.7 as these are applicable to the operation of high pressure storage tanks at hydrogen refueling stations.

Fatigue crack growth rate testing was performed in air and high purity (99.9999%) high pressure hydrogen gas, respectively. Due to the time required to acquire these data sets, a single test was performed at each stress ratio and environmental condition (e.g. air or H_2). For tests performed in air, humidity values were not specifically recorded but range from 30-60% in our laboratory. For tests performed in gaseous H_2, samples were placed in a custom-build pressure vessel, which is located in a servo-hydraulic load frame. The high pressure testing system is equipped with dynamic seals to allow for concurrent loading while under pressure. More details on the specifics in the testing capabilities are available in Ref. [4]. Tests were performed at 293 K and at pressure of either 21 or 100 MPa H_2. Maintaining a good seal is critical to accomplishing long-term tests; higher pressures combined with high frequencies generate significant wear on the seals that can result in shorter seal lifetimes and force tests to be terminated prematurely. The consequence is that only a single test was completed at 100 MPa H_2. The remainder of the tests were performed in gaseous hydrogen at pressure of 21 MPa, which preserved the intergrity of the pressure seals over the course of the test.

Prior to starting any test in high pressure hydrogen gas, the system was leak checked at test pressure with helium, followed by four successive purges with nitrogen to a pressure of 14 MPa, and four successive purges with hydrogen to a pressure of 14 MPa. The system was then filled to the test pressure and the transducers could equilibrate (typically 48 hr) before starting the test. Typical values of oxygen and water measured in gas samples extracted from the test volume at the conclusion of the test are below 1 and 5 vppm, respectively. Load-line displacement was measured with a strain-based clip gauge attached to the sample and load was measured with an internal load cell also on the load-line. Load, crack length, and crack opening displacement were recorded every 0.05 mm using the compliance method with the aid of Fracture Technology Associates (FTA) fatigue crack growth rate software [5].

The crack growth rate (da/dN) as a function of stress intensity factor (ΔK) was calculated following a seven

point polynomial method outlined in ASTM E647 [2]. At the completion of the tests, the samples were broken in half by fatigue cycling in air to allow inspection of the fracture surfaces. Optical measurements were used to correct the crack lengths determined from the measured unloading compliance. The ΔK was corrected for crack closure via the adjusted compliance ratio (ACR) method described in [6] and applied through the FTA software [5]. Plots of FCGR are described as da/dN vs ΔK_{ACR} to acknowledge that the data were corrected for crack closure.

Figure 2 shows an optical image of the fracture surface from an X100 specimen. Within the precrack region, a small (lighter colored) region can be observed, which represents a small crack that extended during the compression-compression precracking. The majority of the precrack (~5 mm) was generated by the tension-tension precracking. Crack extension in 21 MPa H_2 is clearly observable and two regions are distinguishable representing cycling at stress ratio of R=0.5 and R=0.7, respectively. A rising-displacement fracture test was completed in 21 MPa H_2 following the fatigue test, which shows an extremely rough surface. The results of the fracture toughness tests are not discussed further in this paper. Overall, uniform crack fronts were observed in the tested materials as shown in Fig. 2.

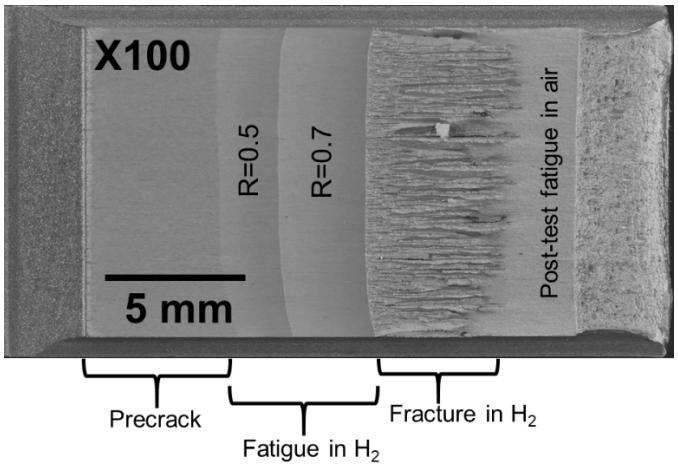

Figure 2 – Optical image of fractured X100 specimen. There are several distinct regions observable on the fracture surface: precrack in air, K-shed at R=0.5 in H_2, K-shed at R=0.7 in H_2, fracture test in H_2, followed by post-fatigue in air to separate the specimen.

RESULTS

Fatigue crack growth rate tests at low ΔK

Fatigue crack growth rates were measured in both air and high pressure hydrogen gas at stress ratios of R=0.5 and R=0.7 on the same sample. The focus was to measure da/dN at lower ΔK ranges; however, as da/dN decreases the test duration can become exceedingly long. To enable testing in a practical amount of time, a test frequency of 10 Hz was utilized for ΔK less than about 7 MPa $m^{1/2}$. Figure 3a shows the FCGR curves (da/dN vs ΔK) of X100 steel tested in both air and 21 MPa H_2. Fatigue cycling in hydrogen at ΔK greater than 7 MPa $m^{1/2}$ was performed at 1 Hz. At ΔK values greater than 8 MPa $m^{1/2}$, the slope of the FCGR curve in hydrogen is clearly steeper compared to the FCGR curve in air. At ΔK less than 6 MPa $m^{1/2}$, the curves overlap to some extent, but it appears that the FCGR in hydrogen is lower than the FCGR in air. The influence of stress ratio (R) is observed in the curves: the higher stress ratio results in higher FCGR for a given ΔK [7]. This trend is observed, for the most part, across the entire ΔK range tested. Also shown in Fig. 3a are the design curves as stated in the ASME BPVC Code Case 2938 for R of 0.5 and 0.7 respectively, which have been approved for use with ASME SA-372 and SA-723 steels for construction according to ASME BPVC Section VIII, Div 3 for operating pressures up to 103 MPa H_2. Although these curves are currently limited to use for SA-372 and SA-723, the curves have been shown to capture the behavior of a variety of ferritic steels [1] and provide a common FCGR reference in Figures 3-5.

Even at high stress ratio (e.g., 0.5 and 0.7), low ΔK tests are still susceptible to crack closure. To account for potential crack closure, the adjusted compliance ratio (ACR) was used to correct for crack-closure effects. Figure 3b shows the crack growth rates (da/dN) versus the closure corrected stress intensity factor range (ΔK_{ACR}). The curves tested at stress ratio of 0.5 are more likely to exhibit crack closure than tests at R=0.7. The difference in closure becomes obvious when comparing the FCGR curves in Fig. 3a and Fig. 3b, as the FCGR curves for R=0.5 shift when corrected for closure, whereas the curves for R=0.7 exhibit a negligible shift. After correction for closure, the FCGR curves in air and H_2 (Fig. 3b) show more overlap at low ΔK than prior to the closure correction.

As stated previously, the design curves were developed from data generated at higher ΔK where closure effects are insignificant. Extrapolation of the design curves, then presumes no crack closure. To demonstrate the effects of closure, two plots are shown for each tested steel: 1) da/dN vs ΔK, which does not correct for closure, and 2) da/dN vs ΔK_{ACR}, where the closure correction is applied. Comparisons between dry hydrogen and moist air are expected to result in differences in closure behavior, so correction for closure is helpful for comparison of these

two environments. It allows for separation of intrinsic effects due to hydrogen compared to extrinsic effects such as remote closure.

ASTM E647 [2] defines an operational ΔK_{th} as the FCGR at 10^{-10} m/cycle. Although it does not appear that a true ΔK_{th} is attained in our data sets, the operational ΔK_{th} for the tests performed in hydrogen fall between 3 and 4 MPa $m^{1/2}$. The operational ΔK_{th} is observed to be lower for the higher stress ratio of R=0.7, as expected. For subsequent discussion, we use this operational definition for the fatigue threshold intensity factor range: $\Delta K_{th.}$

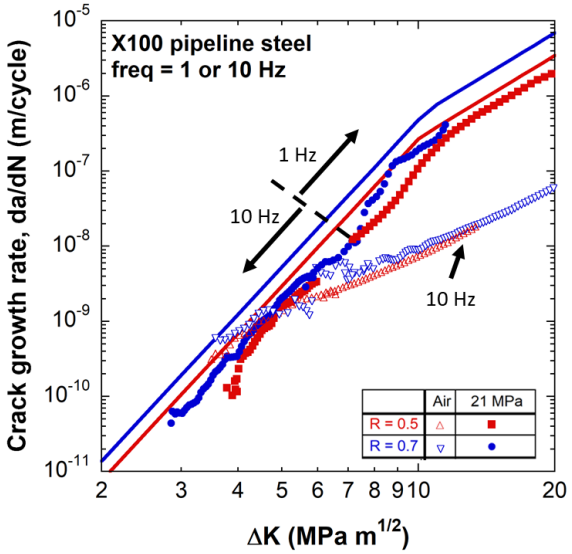

(a)

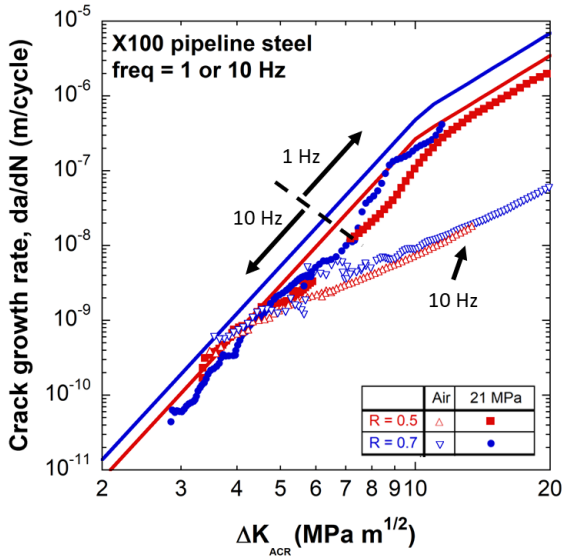

(b)

Figure 3 – (a) Fatigue crack growth rate (da/dN vs ΔK) curves of X100 pipeline steel tested in air and 21 MPa H_2. (b) Fatigue crack growth rate curves (da/dN vs. ΔK_{ACR}) corrected for crack closure. The tests at R=0.5 exhibit greater shifts than R=0.7 if compared to (a). Also, the shift appears to be more significant in H_2 than in air data.

Figure 4a shows the FCGR curves (da/dN vs ΔK) for ASME SA372 Grade J tested in air, 21 MPa H_2, and 105 MPa H_2. Tests were conducted at 10 Hz and at stress ratio of R=0.5 and R=0.7, respectively. For comparison, ASTM A372 Grade N Class 100 data are shown in air tested at R=0.7. Both SA372 Grade J and A372 Grade N show very similar behavior in air at R=0.7. The single test performed in 105 MPa H_2 at R=0.5 exhibits a higher FCGR than the 21 MPa H_2 test in the low ΔK range (e.g. 4-5 MPa $m^{1/2}$). It is commonly observed that higher pressures result in higher FCGR in lower ΔK range (e.g. > 6 MPa $m^{1/2}$) [8]. The effect of hydrogen pressure is neglible in the higher ΔK range, namely above the knee as described in [1]. Similar to the X100 steel, at low ΔK, the FCGR of SA372 Gr. J in H_2 falls below the FCGR in air (Fig. 4a), particularly for the data with R=0.5. When corrected for closure (Fig. 4b), the differences between the FCGR in air and H_2 at low ΔK diminish, and FCGRs tend to follow the design curves. The ΔK_{th} values were measured to be between 3-4 MPa $m^{1/2}$, similar to the ΔK_{th} of X100. The design curves capture the FCGR behavior very well over the entire ΔK range in Fig. 4b.

Figure 5a shows FCGR curves of the 4130X steel, which is used to fabricate conventional laboratory gas cylinders (DOT-3AAX). FCGR tests were performed in air and 21 MPa at a frequency of 10 Hz and at stress ratio of R=0.5 and R=0.7, respectively. Shifts in the FCGR curves of 4130X for closure correction is less noticeable (Figure 5b) than for the other materials. The da/dN of 4130X in H_2 consistently falls below the air data when ΔK is less than 5 MPa $m^{1/2}$. The design curves provide a conservative upper bound for the 4130X steels tested in 21 MPa H_2.

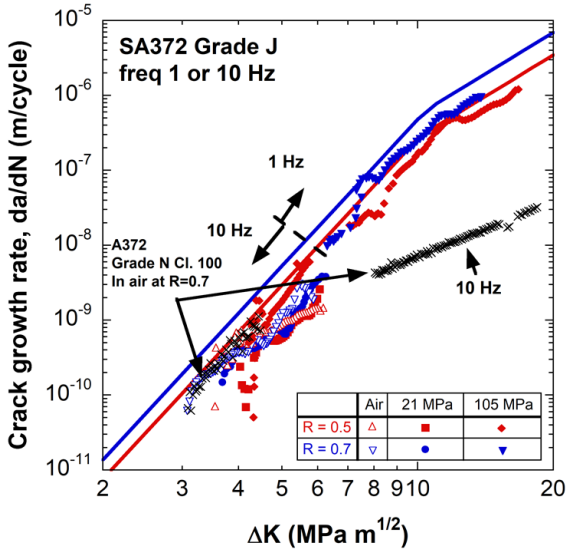

(a)

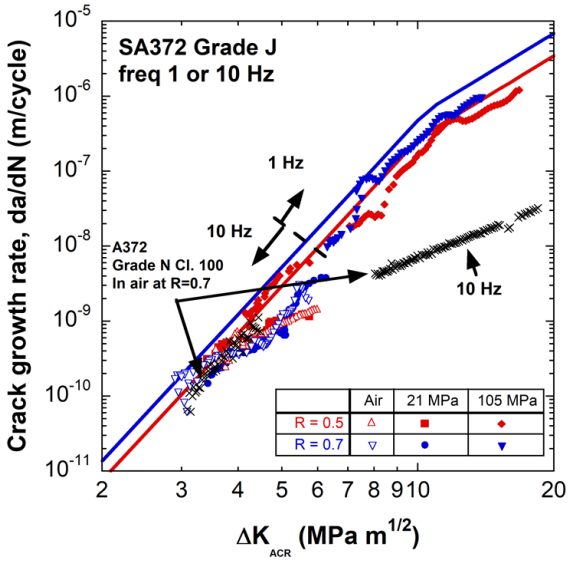

(b)

Figure 4 – (a) Fatigue crack growth rate (da/dN vs. ΔK) curves of ASME SA372 Grade J pressure vessel steel tested in air, 21 MPa H_2, and 105 MPa H_2. Also shown are ASTM A372 Grade N Cl. 100 tested at R=0.7 in air. (b) Fatigue crack growth rate curves (da/dN vs. ΔK_{ACR}) corrected for crack closure.

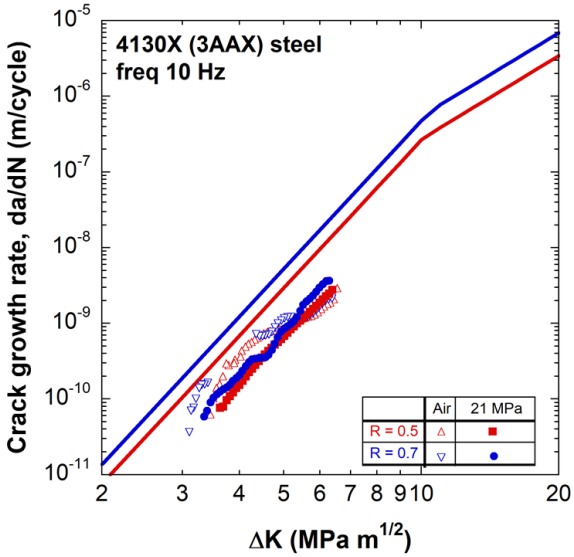

(a)

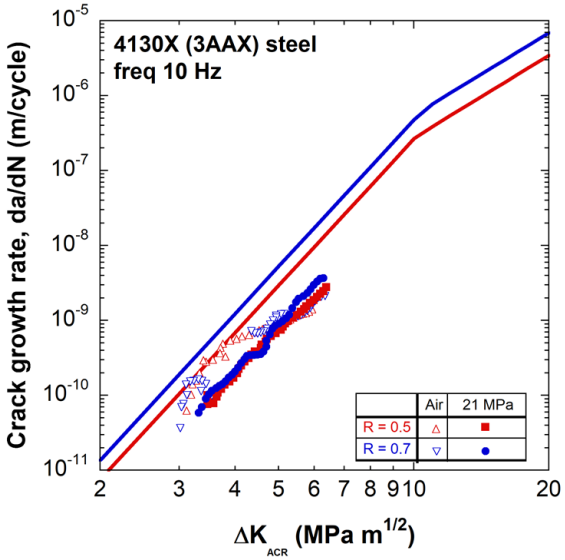

(b)

Figure 5 – (a) Fatigue crack growth rate (da/dN vs. ΔK) curves of 4130X steel tested in air and 21 MPa H_2 at stress ratios of R=0.5 and 0.7. (b) Fatigue crack growth rate curves (da/dN vs. ΔK_{ACR}) corrected for crack closure.

Fracture surfaces of fatigue samples

Select samples of the X100 pipeline specimens were examined in a scanning electron microscope to observe features on the fracture surfaces. The results are shown in Fig. 6 for X100 tested in 21 MPa H_2 at a stress ratio of R=0.5. The crack growth directions in all the fracture surface images is from bottom to top of the images. Figure 6a shows the fracture surface corresponding to ΔK of ~3.8

MPa $m^{1/2}$ and features fatigue striations commonly observed in ferritic steels tested in an air environment. An enlarged image is shown in Fig. 6a with white arrows pointing to the rough striations. Figure 7 shows these fatigue striations very clearly on the fracture surface of an X52 pipeline steel tested in air at $\Delta K \sim 8$ MPa $m^{1/2}$ and is representative of the typical features on fracture surfaces of ferritic steels when tested in air. The white arrows in both Fig. 6a and Fig. 7 point to perturbations on fracture surfaces that appear to be striations that suggest a blunting and resharpening during crack growth.

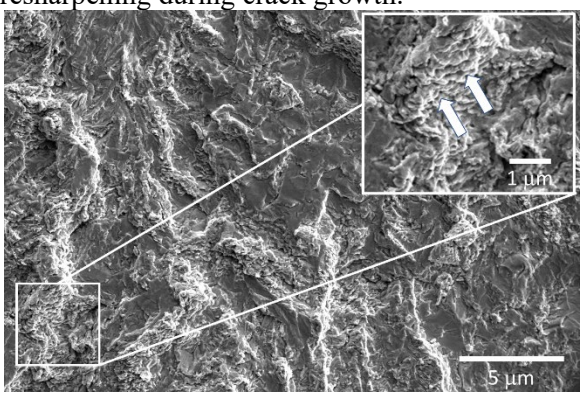

(a)

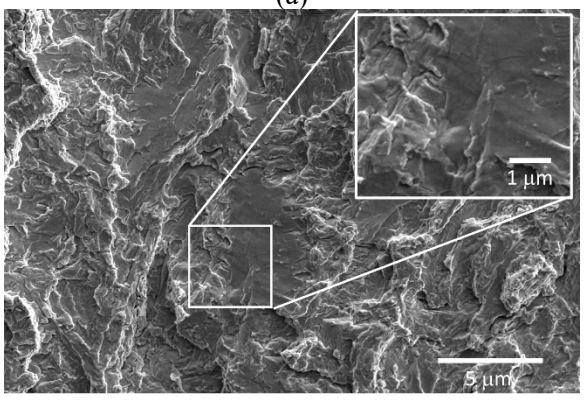

(b)

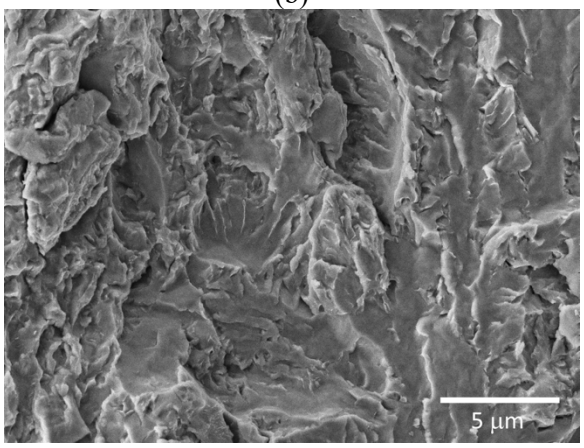

(c)

Figure 6 – Scanning electron microscope images of X100 fracture surfaces for FCGR tests performed in 21 MPa H_2 at stress ratio R=0.5: (a) $\Delta K \sim 3.8$ MPa $m^{1/2}$, (b) $\Delta K \sim 6$ MPa $m^{1/2}$, (c) $\Delta K > 15$ MPa $m^{1/2}$. The arrows in (a) point to fatigue striations.

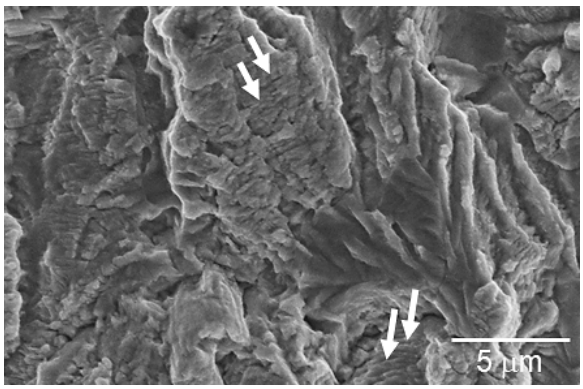

Figure 7 – Scanning electron microscope image of X52 pipeline steel fatigue tested in air a $\Delta K \sim 8$ MPa $m^{1/2}$. Arrows point to fatigue striations.

Figure 6b shows the fracture surface of X100 pipeline steel tested in 21 MPa H_2 at a $\Delta K \sim 6$ MPa $m^{1/2}$. The characteristic features on the fracture surface are larger, flat regions with less roughness overall. The enlarged region shows that there is a noticeable absence of striations. Figure 6c shows the X100 pipeline steel at higher $\Delta K > 15$ MPa $m^{1/2}$ in 21 MPa H_2. The features in Fig. 6c are consistent with the lack of striations in Fig. 6b.

DISCUSSION

Three different ferritic steels were tested at low ΔK (<6 MPa $m^{1/2}$) in high pressure hydrogen gas at R=0.5 and R=0.7. The tests conducted in this work highlight consistent trends among all three steels as will be discussed further; however, it is important to note that more testing is needed before these trends can be generalized for behavior in the low ΔK range. Similar to trends observed at higher ΔK [1], FCGRs are remarkably similar in the near threshold regime for the steels in this study. Although a finite ΔK_{th} was not apparent (e.g. indicated by da/dN rapidly tending toward zero), data were generated for FCGRs less than 10^{-10} m/cycle, which is commonly deemed an operational threshold [2]. Using this operational definition of threshold, ΔK_{th} measured for the ferritic steels ranged between 3 and 4 $MPa^{1/2}$. Previous data generated at only higher ΔK often speculated that the hydrogen curves would decrease to da/dN values similar to in air at lower ΔK [9-11]. When corrected for closure, the X100 (Fig. 3b) and SA372 Grade J (Fig. 4b) show

consistent FCGR between air and hydrogen environments. The 4130X steel differs from the other steels in that the FCGR curves for 21 MPa H_2 fall below the air curves for both R=0.5 and R=0.7. The reason for this is not clear.

The convergence of the FCGR in air and H_2 at low ΔK and high R, similar to the X100 and SA372 Grade J, has been observed previously [7], albeit at low pressures. At low ΔK, the effects of hydrogen are diminished [7] and hydrogen acts effectively as inert gas, providing an oxygen and moisture free environment and suppressing oxide-induced closure. Since the applied ΔK is higher than the effective ΔK when load can be transferred in the wake of the crack due to closure, tests in air (especially at lower stress ratios) result in higher ΔK_{th} when not corrected for closure [7]. Interestingly, both with and and without a correction for closure, the operational ΔK_{th} for the 4130X was lower in air than in hydrogen, contrary to the anticipated effect of an oxide-induced closure. One possibility is that humidity from the air was contributing hydrogen to the crack tip offsetting the contribution of closure. It should also be noted that these results represent single (difficult to execute) tests. More testing is needed to clarify if this trend for 4130X is repeatable and, if so, the origin of this unusual behavior.

The striations observed in Fig. 6a indicate a blunting and resharpening mechanism is occurring, which is commonly observed on fracture surfaces in air (Fig. 7). Striations are not conventionally observed in tests in H_2 on ferritic steels [10, 11] when tested at higher ΔK when crack growth rates are higher. Striations observed on the fracture surface near ΔK_{th} in H_2 are likely the result of the diminished effect of hydrogen when ΔK is low, mentioned above. Conventional fatigue crack evolution occurs via a blunting and resharpening mechanism that results in striations as commonly observed in air, especially at low ΔK when crack growth rates are low. At low ΔK, where hydrogen does not have a strong effect on FCGR, this same basic process seems active as demonstrated by the striations in Fig 6a. However, hydrogen limits plasticity, thus at high ΔK (where the plastic zone is larger) blunting is suppressed, inducing a sharper crack tip. Thus, at higher ΔK in hydrogen, the formation of striations is also suppressed.

The test frequency of 10 Hz was used for the ΔK_{th} experiments to enable completion of the tests in a reasonable amount of time. Tests in hydrogen gas as a function of frequency have been examined at higher ΔK ranges [9], which showed less than a factor of 2-3 lower FCGR at 10 Hz compared to 1 Hz. At lower frequency, the effect of frequency on FCGR diminished. The effect of frequency is generally related to time scales for hydrogen transport and can be related to the rate of crack growth with time ($da/dt = f \times (da/dN)$). Thus, the rate of crack extension (da/dt) near ΔK_{th} at 10 Hz will still be much lower than at ΔK = 8 MPa $m^{1/2}$ at 1 Hz. In other words, the effect of frequency should diminish as da/dN tends toward threshold and tests near threshold can be executed at higher frequency. This concept is supported by the observation that extrapolation of the data generated at 1 Hz at higher ΔK adequately bounds the data generated at 10 Hz at lower ΔK. This suggests that test frequency plays less of a role near ΔK_{th} than at ΔK of 10 or 20 MPa $m^{1/2}$. Given the known role of trace oxygen impurities and their effects on FCGR [10], it is important to note that oxygen impurities will likely have a much stronger effect on ΔK_{th} measurements in hydrogen than in other regions of the FCGR curve.

The design curves from ASME Code Case 2938 for R=0.5 and R=0.7 provide an upper bound curve for all the data generated in this paper. The design curves provided a better fit to the closure corrected data, as anticipated, suggesting that the FCGR behavior in hydrogen does not change in the low FCGR regime for ΔK as low as about 4 MPa $m^{1/2}$. These data further imply that the design curves provide a conservative estimate of the FCGR in hydrogen for ΔK as low as the operational ΔK_{th} of 10^{-10} m/cycle. This observation strengthens the integrity and value of the design curves over the full range of relevant FCGRs. In most cases, pressure vessels and pipes operate at low ΔK for the majority of their life, and in the case of autofrettaged vessels the effective ΔK may be in the threshold regime. Thus, data in hydrogen near ΔK_{th} enables design of longer-life pressure components with greater confidence. The fact that the FCGRs in hydrogen appear to become coincident or below those in air could perhaps influence future designs and reduce overly conservative safety margins.

SUMMARY

Fatigue crack growth rates of ferritic steels were measured at low ΔK in high-pressure hydrogen gas and in air at stress ratio of R=0.5 and R=0.7, respectively. FCGR curves in hydrogen appeared to be coincident or below the curves in air at ΔK < 5 MPa $m^{1/2}$. This result is surprising as moisture from the air would be expected to contribute to oxide-induced closure, resulting in the retardation of FCGRs in air (whereas hydrogen is expected to display minimal closure due to the lack of moisture and air). A modest amount of closure was observed in the hydrogen FCGR curves tested at the low ΔK, particularly at R=0.5.

The adjusted compliance ratio (ACR) correction was applied to account for crack closure in all cases. Closure-corrected FCGR curves (da/dN vs. ΔK_{ACR}) in hydrogen are comparable to the ASME design curves, and consistent with the FCGR in air in the low ΔK range. Operational ΔK_{th} (e.g. da/dN ~ 10^{-10} m/cycle) was measured between 3 and 4 MPa $m^{1/2}$ and exhibited remarkable consistency between the tested pressure vessel steels (SA372 and 4130X) and pipeline steel (X100). The design curves from ASME Code Case 2938 provided an upper bound for the data and captured the behavior in the ΔK_{th} demonstrating the utility of the design curves over a broad range of ΔK. Near ΔK_{th}, the fracture surfaces exhibited fatigue striations which are commonly observed in tests in air, but are typically absent in hydrogen environments where crack growth rates are accelerated. The effect of hydrogen appears to be diminished in the low ΔK range indicated by the similar da/dN values and similar fracture appearance to the tests performed in air.

ACKNOWLEDGMENTS

The authors are grateful to B. Davis and J. McNair for support of high pressure testing, A. Gardea, H.Vega for metallographic preparation, and W. York and R. Nishimoto for SEM imaging. Sandia National Laboratories is a multimission laboratory managed and operated by National Technology and Engineering Solutions of Sandia, LLC., a wholly owned subsidiary of Honeywell International, Inc., for the U.S. Department of Energy's National Nuclear Security Administration under contract DE-NA-0003525.

Table 1 – Chemical Compositions for Steels (in wt%)

	Cr	Mo	Mn	Si	C	Fe
X100	0.19	0.17	1.69	0.26	0.085	Bal
SA372 Gr. J	0.99	0.18	0.93	0.28	0.49	Bal
4130X	0.95	0.18	0.63	0.28	0.30	Bal
A372 Gr. N	0.8-2	0.2-0.4	< 0.90	< 0.35	< 0.35	Bal

REFERENCES

[1] C. San Marchi, J. Ronevich, P. Bortot, Y. Wada, J. Felbaum, and M. Rana, "Technical basis for master curve for fatigue crack growth of ferritic steels in high-pressure gaseous hydrogen in ASME Section VIII-3 code PVP2019-93907," presented at the Proceedings of the ASME 2019 Pressure Vessels & Piping Conference, San Antonio, TX, July 14-19, 2019.

[2] *E647-11 Standard Test Method for Measurement of Fatigue Crack Growth Rates*, ASTM, West Conshohocken, PA, 2011.

[3] J. C. Newman and Y. Yamada, "Compression precracking methods to generate near-threshold fatigue-crack-growth-rate data," *International Journal of Fatigue,* vol. 32, no. 6, pp. 879-885, 2010/06/01/ 2010, doi: https://doi.org/10.1016/j.ijfatigue.2009.02.030.

[4] B. P. Somerday, J. A. Campbell, K. L. Lee, J. A. Ronevich, and C. San Marchi, "Enhancing safety of hydrogen containment components through materials testing under in-service conditions," *International Journal of Hydrogen Energy,* vol. 42, pp. 7314-7321, 2017, doi: 10.1016/j.ijhydene.2016.04.189.

[5] *Fracture Technology Associates (FTA) software*. (2015).

[6] J. K. Donald, "Introducing the compliance ratio concept for determining effective stress intensity," *International Journal of Fatigue,* vol. 19, no. 93, pp. 191-195, 1997, doi: http://dx.doi.org/10.1016/S0142-1123(97)00024-8.

[7] S. Suresh and R. O. Ritchie, "Mechanisitic dissimilarities between environmentally influenced fatigue-crack propagation at near-threshold and higher growth rates in lower strength steels," *Metal Science,* vol. 16, pp. 529-538, 1982.

[8] C. San Marchi, B. P. Somerday, K. A. Nibur, D. G. Stalheim, T. Boggess, and S. Jansto, "Fracture and Fatigue of Commercial Grade API Pipeline Steels in Gaseous Hydrogen," presented at the ASME 2010 Pressure Vessels & Piping Division, Bellevue, Washington USA, 2010.

[9] B. Somerday, P. Bortot, and J. Felbaum, "Optimizing measurement of fatigue crack growth relationships for Cr-Mo pressure vessel steels in hydrogen gas," presented at the ASME 2015 Pressure Vessels and Piping Conference, Boston, MA, July 19-23, 2015, 2015.

[10] B. P. Somerday, P. Sofronis, K. A. Nibur, C. San Marchi, and R. Kirchheim, "Elucidating the variables affecting accelerated fatigue crack growth of steels in hydrogen gas with low oxygen concentrations," *Acta Materialia,* vol. 61, no. 16, pp. 6153-6170, 2013, doi: http://dx.doi.org/10.1016/j.actamat.2013.07.001.

[11] J. A. Ronevich, B. P. Somerday, and C. San Marchi, "Effects of microstructure banding on hydrogen assisted fatigue crack growth in X65 pipeline steels," *International Journal of Fatigue,* vol. 82, no. Part 3, pp. 497-504, 2016/01/01/ 2016, doi: https://doi.org/10.1016/j.ijfatigue.2015.09.004.